energies

MDPI

Article

Mineralogy and Permeability of Gas and Oil Dolomite Reservoirs of the Zechstein Main Dolomite Basin in the Lubiatów Deposit (Poland)

Ewa Krogulec *, Katarzyna Sawicka, Sebastian Zabłocki and Ewa Falkowska

Faculty of Geology, University of Warsaw, Żwirki i Wigury 93, 02-089 Warszawa, Poland; sawicka@uw.edu.pl (K.S.); s.zablocki@uw.edu.pl (S.Z.); ewa.falkowska@uw.edu.pl (E.F.)

* Correspondence: ewa.krogulec@uw.edu.pl; Tel.: +48-22-5540526

Received: 28 October 2020; Accepted: 3 December 2020; Published: 5 December 2020

Abstract: Permeability characterizes the ability of rocks to store and transport natural gas, crude oil and reservoir fluids. Permeability heterogeneity of reservoir rocks, including dolomites, results from overlapping geological and physicochemical processes. The permeability study of gas-bearing dolomites was carried out on the Lubiatów hydrocarbon deposit (Poland), located at the Ca2 carbonate platform toe-of-slope, which is a prospective area for hydrocarbon exploration in Europe. Due to the complicated rock textures and overlapping alteration processes, including secondary crystallization or dissolution of minerals, the permeability of the deposit is variable. Studies of dolomites from a depth of 3242–3380 m show high mineralogical diversity; the percentage of dolomite ranges from 79% to 95% with a variable content of other minerals: anhydrite, gypsum, quartz, fluorite, plagioclase and clay minerals. The porosity variability ranges from 4.69% to 31.21%, depending on the measurement method used. The mean permeability value is 35.27 mD, with a variation range of 0.9 to 135.6 mD. There is neither change in permeability with depth and mineral composition, nor a direct relationship between porosity and permeability.

Keywords: permeability; mineralogy; hydrocarbon deposit; dolomites; Poland

1. Introduction

Permeability is one of the most important petrophysical parameters of reservoir rocks for hydrocarbon accumulations, determining the feasibility of their extraction. Permeability characterizes the ability of rocks to store and transport natural gas, crude oil and reservoir fluids. Permeability quantification of reservoir rocks is also important from the point of view of forecasting its changes resulting from drilling techniques for deposit completion and intensification of hydrocarbon extraction. In reservoir rocks, at a depth of several thousand meters, such as limestone, dolomite, sandstone and shale, which are characterized by very low permeabilities, the permeability quantification consists practically in determining the value relative to other rock characteristics, also determined pointwise or indirectly. Due to the relationships that are difficult to parameterize, permeability is included in a group of fuzzy data [1].

Sedimentation, diagenesis and tectonic movements all play roles in the formation of carbonate reservoirs, the storage space of which is composed of pores, vugs and fractures of different scales [2–5]. Therefore, permeability variations in dolomites are commonly related to the original depositional textures, grain types, stratigraphic position, or paleogeographic location [6–13]. The heterogeneity of permeability values, results from the texture of rocks and the overlapping transformation processes (including secondary crystallization or dissolution of minerals) requires detailed analysis.

The Lubiatów hydrocarbon deposit, located at the Ca2 carbonate platform toe-of-slope [14], was analysed for permeability and other petrophysical parameters of gas-bearing dolomites. Natural gas

is extracted from the Lubiatów deposit at the Lubiatów-Międzychód-Grotów (LMG) production facility, which is the largest natural gas mine in Poland [15]. The gas field is located in an area prospective for hydrocarbon exploration in Europe [16,17].

The aim of the research was to quantify the permeability of the Ca2 dolomites in the deposit and to estimate the permeability heterogeneity. Analysis of the permeability–porosity and permeability–mineral composition relationships was carried out. Results of laboratory tests were compared with results of geophysical measurements and historical laboratory tests in order to quantify the permeability variability, depending on the depth and measurement method. The research results were compared with results of a few studies on permeability of dolomites in other hydrocarbon deposits around the world.

2. Location of the Hydrocarbon Deposit

In Poland, 298 natural gas deposits with total reserves amounting to about 66.64 bcm (66,640.98 million m^3; (compared to the Poland annual consumption of 20.4 bcm in 2019) have been identified and documented. In the Polish Lowlands, 153 natural gas deposits have been discovered [18] with total economic reserves amounting to 19 bcm (19,006.34 million m^3), while the production was about 0.74 bcm (738.39 million m^3). The reserves documented in the Lubiatów natural gas deposit, located in the Polish Lowlands, are 0.61 bcm (612.45 million m^3), while the gas production from the deposit is 0.23 bcm (232.71 million m^3) [18].

The number of documented oil deposits is 86, including 43 oil fields in the Polish Lowlands, which are of the greatest economic significance, as their resources constitute 66% of all Poland's oil resources. The Lubiatów crude oil deposit is one of the 43 fields located in the Polish Lowlands, with documented reserves amounting to 1438.68 thousand tonnes, and the production of 337.49 thousand tonnes (i.e., 2.565 Mbbl) [18]. Several oil provinces have been identified in Poland. The Wielkopolska Petroleum Province, where the Lubiatów field is located, comprises a basinal zone and the southern toe-of-slope of the in the Zechstein Main Dolomite carbonate platform (Figure 1) [19–25]. The Main Dolomite is a prospective oil and gas level in the Polish Lowlands [23,26–30]. The Lubiatów deposit is exploited by the Lubiatów-Międzychód-Grotów (LMG) production facility, which is the largest natural gas "mine" in Poland [15]. Due to its depositional location, the Lubiatów deposit is characterized by a significant diversity of sediments in the vertical section and between individual wells [31,32].

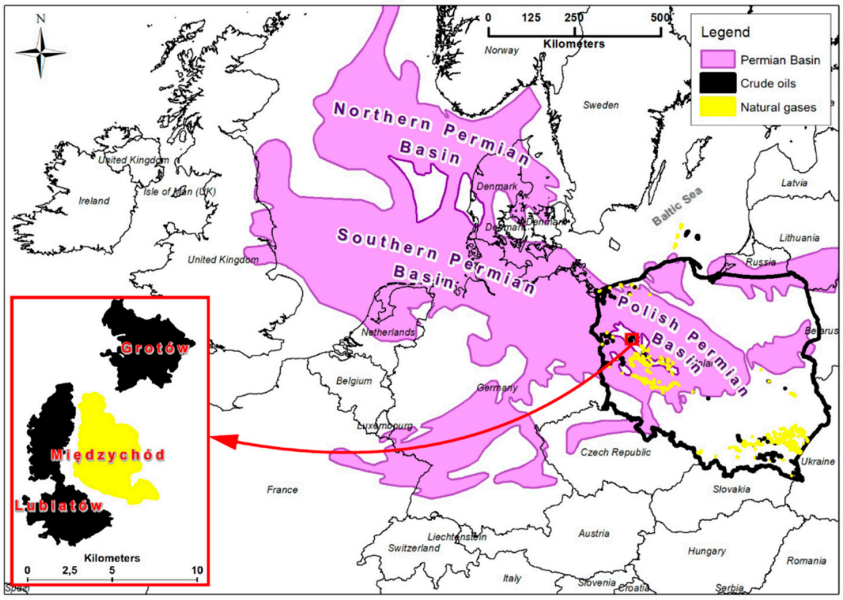

Figure 1. Location of the Zechstein Main Dolomite Basin.

The Lubiatów deposit is developed into 17 wells, comprising vertical, directional, under development, intended for water formation injection, and others [33].

Facies and sedimentological analysis of oil and gas deposits in the Zechstein Main Dolomite (Ca2) of the Polish Lowlands was the basis for the identification of depositional environments represented by zones and subfacies, characterized by different volumetric and permeability features [21–23]. Sedimentation of the Main Dolomite took place in five zones that differed in lithofacies characteristics: in a deep-water zone, local shallows, fore-barrier zone, barrier zone, and lagoonal zone. Three basic subfacies types characterized by different petrophysical parameters are distinguished within them [12,21,22,24]:

(1) boudstones (mainly sublittoral carbonate muddy sands; also carbonate sands and carbonate sandy muds);
(2) mud-supported rocks, i.e., mudstones, wackestones and packstones with abundant bioclasts (mainly dark grey sublittoral carbonate sandy muds and carbonate muds; carbonate muddy sands and microbial sediments being frequent);
(3) grain-supported rocks, i.e., packstones, grainstons, floatstones and rudstones (carbonate sands and muddy sands, carbonate sandy muds and muds).

The primary porosity and permeability of the carbonates have been reduced by secondary diagenetic processes, which is typical for Ca2 deposits. The Main Dolomite is a closed petroleum system where source rocks and reservoirs occur in the same place or in close proximity. The Main Dolomite sections in the Lubiatów deposit are characterized by similar lithologic types [25]; the deposits are represented mainly by rhytmic carbonate muds and carbonate sands and gravels [34]. In other deposits of the Polish Lowlands, the thickness and lithologic-facies variability in individual depositional environments is much greater [14,31].

3. Research Material and Methods

3.1. Research Material

Samples for laboratory analyses were collected from drill cores of three wells from the Lubiatów deposit: Well 1 (L1)—three samples from 3273.35–3283.90 m depth, Well (L2)—two samples from the 3274.32–3275.95 m depth interval, and Well 2k (L2k)—five core samples from a depth interval of 3356.85–3369.60 m (Table 1 and Figure 2). The distance between the wells is proximately 500 m.

Table 1. Summary of the samples.

No	Sample No	Cored Interval (m)	Sampling Depth (m)
		Well 1 (L1)	
1	L1/2	3266–3278	3273.35–3273.45
2	L1/1	3278–3292	3283.80–3283.90
		Well 2 (L2)	
3	L2/1	3265.5–3283	3274.32–3274.42
4	L2/3	3265.5–3283	3275.85–3275.95
5	L2/2	3265.5–3283	3276.90–3277.00
		Well 2k (L2k)	
6	3/3 kw	3348–3361	3356.85–3356.95
7	5/5 w	3348–3361	3357.32–3357.42
8	4/4 w	3361–3366	3361.20–3361.30
9	2/2 s	3366–3375	3367.17–3367.27
10	1/1 kw	3366–3375	3369.50–3369.60

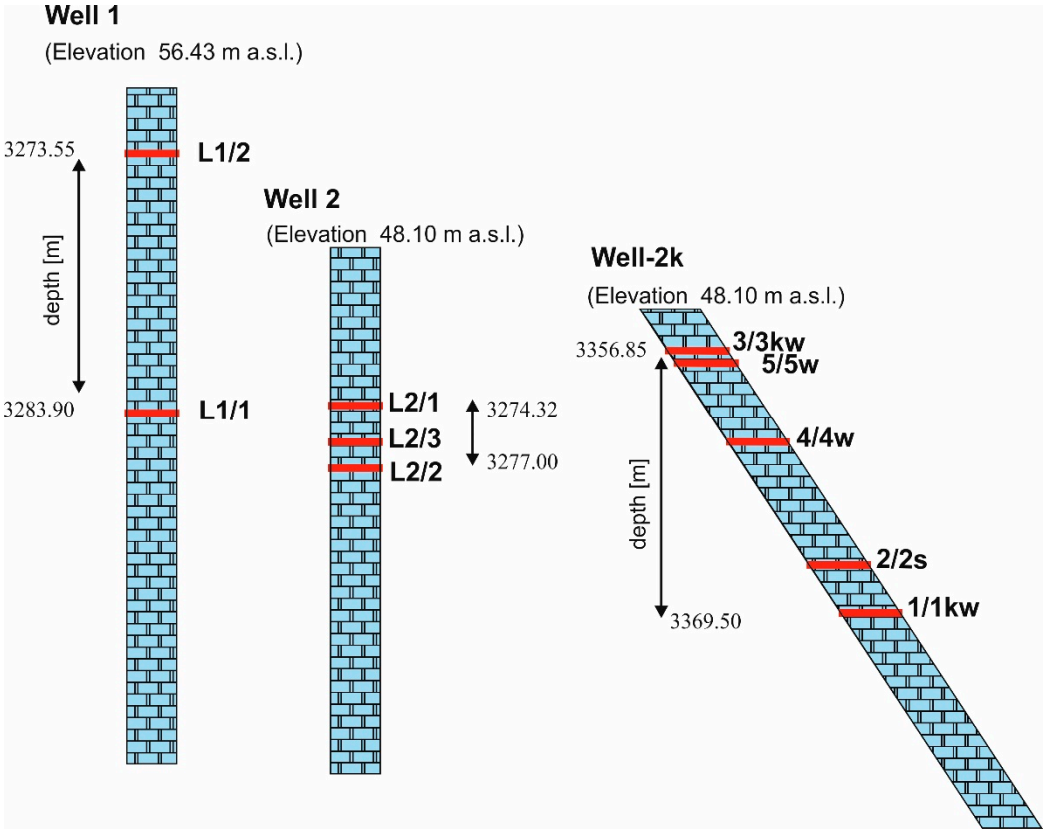

Figure 2. Location of samples from well profile parts.

The limited number of samples results from the difficulty of accessing drill cores acquired in previous years and from legal restrictions. In accordance with the Geological and Mining Law of Poland [35] and the ordinances of the Minister of the Environment, samples not less than $\frac{1}{2}$ of the core diameter are archived by the Polish Geological Survey, as in other countries, which results from the principle of preservation and access to geological information.

3.2. Study of Research

Study of permeability of dolomites can be described on different scales:

- mineral grains (nano and micro scale);
- lithology packages (millimetre and centimetre scale);
- drill core study (centimetre scale);
- sedimentary complexes, lithological variability, models (regional scale).

Permeability measurements in reservoir rocks for hydrocarbon accumulations are most often carried out indirectly, by interpreting results of geophysical investigations in wells, e.g., nuclear magnetic resonance (NMR), resistivity profiling, radiometric methods using neutron-gamma (NEGR) or neutron-neutron (NN) logs, and formation tests, e.g., on the basis of formation pressure build-up [36–41]. These are regional studies with the possibility of refining them to a more detailed scale.

Direct laboratory centimeter-scale studies of drill cores use porosimetry methods, the flow-pump method [42], and measurements with various types of permeameters, including PDPK-400 of CoreLab Inc., Tulsa, OK, USA [43].

A separate group of methods for quantifying permeability in reservoir rocks is an attempt to parameterize the size, i.e., to obtain the highest correlation coefficients of permeability with more easily and precisely measured parameters [30]. The correlation relationship is determined by

the precision of estimating the values building the relationships; however, the assessment scale of the correlated parameters is often varied. The relationships of permeability or other parameters characterizing reservoir rocks are described in numerous publications (e.g., [5,44–49]). Many methods are based on permeability quantification by determining porosity, pore geometry, sizes, and capillary (e.g., [7,50–55]). Another method that uses data correlation is the measurement of permeability based on the relationship between capillary pressure and NMR [56–58]. The relationship between permeability and the dolomitization process is indirectly determined by the assuming that the dolomitization process increases porosity [59]. This assumption is debated as studies by Schmoker and Halley [60] and Lucia and Major [61] indicate a reduction in porosity during the dolomitization process.

Mineral composition and porosity of the dolomites samples were analyzed using:

1. ZEISS SteREO discovery.v20 optical microscope at a magnification of ×80. Due to the colouring of pores and fractures in the sample, it was possible to calculate the effective porosity of the rock using the image processing program imageJ. By cutting the coloured fields out of the photos obtained, the program calculated their surface areas and thus the effective porosity of samples. The total porosity was also calculated.
2. SEM (scanning electron microscope). Samples for the SEM analysis were sputtered with a thin (approx. 20 nm) carbon layer, allowing the discharge of electric charges accumulating on the surface of the tested sample, and then examined using a SIGMA VP scanning microscope with an EDS detector. The studies were carried out in high vacuum (~5×10^{-5} mbar) ensuring high resolution and quality of the image obtained and a large number of counts on the EDS detector, which results in high quality of mappings (spatial distribution analysis) of chemical elements. The surface area occupied by dark fields in the BSE image, which can be interpreted as pore space/fractures or an area filled with the epoxy resin/cyanoacrylate adhesive used for making thin sections, was automatically counted. It was possible to determine the total and effective porosity.
3. X-ray diffraction (XRD) analysis. Samples were recorded in the range of 4–78° 2θ, with a step of 0.026° 2θ, powder preparations, pressed with the preparation rotation 1 rps, filtered CoKα radiation (Fe filter) with current parameters of 30 mA and 40 kV. Analysis of the results was carried out using the X' Pert HighScore Plus software (ver. 2.2e) and the ICDD PDF-2 Release 2008 RDB database.

3.3. Permeability Measurements

The permeability test was performed with the use of a Micromeritics AutoPore IV 9500 mercury porosimeter. The test procedure was developed on the basis of the standard research protocol published by the American Society for Testing and Materials (ASTM-D4404-10 2010) and the AutoPore IV 9520 Operator's Manual V1.09 2008 prepared by the Micromeritics company. The samples were dried for 24 h at a temperature of about 105 ± 5 °C. The measurements were carried out on the assumption that the sample was evacuated to 50 µm Hg (6.67 Pa) for 50 min and the equilibration time was 60 s. They were made on 120 points in the pressure ranging from 0.5 to 60,000 psi (0.003–413.7 MPa).

The mercury porosimetry method consists in injecting mercury into the pore space of the tested material [62–64]. As a non-wettable liquid, mercury does not spontaneously penetrate the pores of the material; therefore, its intrusion into the pores of the sample requires using appropriate pressure. Injection pressure (capillary) is associated with pore radii by the Washburn formula [65–67], using a cylindrical model of rock pore space:

$$P = 2\sigma cos\theta / r$$

where: P—capillary pressure (Pa), σ—surface tension (N/m), θ—contact angle (°), r—radius of capillary tube (m).

On the basis of the pressure values and the mercury intrusion volume, the measuring apparatus determines the volume of pores and their distribution. The AutoPore IV 9520 [68] can perform analysis up to a pressure of 60,000 psi (414 MPa), making it possible to measure pore diameters in the range of

0.003–500 µm. The AutoPore software converts the volume measurements into measurement points that show the volume of mercury penetrating the pores of the sample.

The relationship between Hg injection curves and permeability has been investigated by a number of authors [69–72]. Analysis of the cumulative curve, identification of the curve irregularity, evaluation of the boundary effect, and determination of the inflection point of the cumulative curve, which represents the value of the threshold pressure from the physical point of view, have been the subjects of many publications (i.e., [30,48,53,56,73–79]). The permeability coefficient value is determined by the Katz–Thomson method, in which the coefficient is calculated according to the formula [75,76]:

$$k = CL_{char}^2 \frac{\sigma}{\sigma_o}$$

where: k—permeability coefficient (mD), σ—electrical permeability of brine-saturated material (mS), σ_o—electrical permeability of brine (mS), C—permeability constant (1/226 = 0.00442), L_{char}—characteristic length of pores (m), determined on the basis of threshold pressure P_{th} and Washburn's equation [80,81].

The threshold pressure value is estimated from the logarithmic differential intrusion curve on which the threshold pressure corresponds to the first distinct point of increase in mercury intrusion. In the case that the σ/σ_o ratio value is not entered, the calculation procedure is based on the following relationship [75,76,80,81].

$$k = \frac{1}{89} L_{max}^2 \frac{L_{max}}{L_{char}} n S_{Lmax}$$

where: L_{max}—maximum length at which the highest permeability occurs (m), S_{Lmax}—volume of effective pores wider or equal to L_{max} (m^3), n—porosity (%).

Analysis of permeability was also performed using a permeameter PDPK-400 produced by PDPK-400 of CoreLab Inc., Tulsa, OK, USA [43]. This apparatus enables permeability profiling of rocks in drill cores of various diameters (minimum 2.5 cm), i.e., from 2.5 cm to 3 m long, from which the average value is calculated. Measurements with the PDPK 400 permeameter practically cannot be used in a wider range due to the sample size.

4. Results

4.1. Mineralogical Composition

Drill core samples collected from a depth of 3242–3380 m of three wells located at a close distance (not more than 2 km) show high diversity, as revealed by macroscopic, XRD, SEM and microscopic investigations (Tables 2 and 3).

Table 2. The characteristics of rock samples from the Well 1, Well 2 and Well 2k wells.

Sample No, Depth (m)	Macroscopic Description	Optical Microscope	X-ray Diffraction XRD	Scanning Electron Microscope SEM
L1/2 3273.35–3273.45	Grey pelite dolomite, porous, with less porous irregular clasts	Fine-grained, equigranular dolomite, highly porous. Pores are usually oval, particularly larger ones.	Dolomite 88%; anhydrite 6%; plagioclase 6%	Dolomite 68.4; quartz 1.03%; plagioclase 4.18%; clay minerals 0.004%.
L2/1 3274.32–3274.42	Grey pelite dolomite, hard, numerous clay-dolomitic laminae, yellow-green oil seeps, bituminous smell	Fine-grained, equigranular dolomite, admixture of anhydrite usually forming large clusters of crystals.	Dolomite 91%; anhydrite 4%; plagioclases 4%; quartz 1%.	Dolomite 72.64–75.08%; anhydrite 0.24–1.33%; fine-grained quartz 0.26–0.52%; clay minerals 0.004–0.01%; traces of feldspars.

Table 2. *Cont.*

Sample No, Depth (m)	Macroscopic Description	Optical Microscope	X-ray Diffraction XRD	Scanning Electron Microscope SEM
L 2/3 3275.85–3275.95	Dark grey dolomite with numerous seeps of green-yellow oil; fine lenses of calcite and sporadically of anhydrite; bituminous smell.	Fine-grained dolomite with anhydrite, high porosity.	Dolomite 94%; anhydrite 1%; plagioclases 5%; quartz 1%.	Dolomite 78.03%; anhydrite 0.88%; fine-grained quartz 0.76%; clay minerals 0.08%
L2/2 3276.90–3277.00	Dark grey dolomite, with numerous seeps of yellow-green oil, lenses of light calcite and sporadically of anhydrite; bituminous smell.	Fine-grained dolomite, porous; fine-grained anhydrite.	-	Dolomite 84.13%; fine-grained anhydrite 0.75%; fine-grained quartz 0.57%.
L1/1 3283.80–3283.90	Pelite dolomite, grey, almost black on a broken rock surface, yellow-green oil shows in some scarce small fractures along cracks.	Fine-grained dolomite with organic debris forming larger clasts containing oval pores, some pores are very large in size.	Dolomite 79%; anhydrite 5%; plagioclases and fluorite 1%.	Dolomite—64.65%; fine-grained quartz 1.25%; anhydrite 4.54%; calcite 0.54%; clay minerals 0.03%; trace amounts of feldspars.
L 2k/3 3356.85–3356.95	Black pelite dolomite, locally fine-grained, distinctly laminated obliquely to the core axis.	Very fine-grained dolomite, distinctly bedded.	Dolomite 95%; anhydrite 2%; plagioclases 1%; quartz 2%.	Very fine-grained quartz, feldspars, fine-grained anhydrite.
L 2k/5 3357.32–3357.42	Grey dolomite, locally finely crystalline, pelitic in places.	Fine-grained dolomite; zones with very fine pores of very irregular shapes are observed.	Dolomite 91%; anhydrite 5%; plagioclases 1%; quartz 1%.	-
L 2k/4 3361.20–3361.30	Grey dolomite, slightly crystalline, finely laminated with pelite dolomite, fractures filled with calcite.	Very fine-grained dolomite; variously sized pores, locally oval.	Dolomite 95%; anhydrite 2%; plagioclases 1%; quartz 1%.	Dolomite 63%; anhydrite 3.68–6.50%, very fine–grained quartz 0.40–4.14%; trace amounts of feldspars and clay minerals.
L 2k/2 3367.17–3367.27	Dark grey dolomite with a beige hue, fine-grained, variably recrystallized; laminated and bedded dolomite, bituminous smell.	Equigranular dolomite; traces of dispersed gypsum.	Dolomite 95%; anhydrite 2%; plagioclases 1%; quartz 1%	Dolomite 83.13%; fine–grained quartz 1.2–1.7%. anhydrite 0.7–1.22%.
L 2k/1 3369.50–3369.60	Dark grey, fine-grained dolomite with a beige hue, variably recrystallized; laminated and bedded dolomite, bituminous smell.	Fine-grained dolomite, organogenic fragments are visible in places, anhydrite in patches, small pores, most often closed.	Dolomite 95%; anhydrite 2%; plagioclases 1%; quartz 1%.	Dolomite 73.32%; quartz 2.10–2.50%; dispersed feldspars; anhydrite 1.33%.

Table 3. Percentages of major minerals in the samples, X-ray diffraction (XRD) method.

Sample No	Dolomite (%)	Quartz (%)	Gypsum (%)	Anhydrite (%)
L 2k/3	91	4.62	1.68	1.97
L 2k/5	81	5.43	4.75	3.94
L 2k/4	89	0.4	6.5	3.68
L 2k/2	97	1.70	1.22	0.7
L 2k/1	76	2.10	1.3	19.43
L 1/2	88	1.03	0.24	4.80
L 2/1	91	0.52	0.08	1.33
L 2/3	94	0.76	0.75	4.02
L 2/2	90	0.57	4.18	0.67
L 1/1	79	1.25	4.54	15.77

The research methods used to determine the mineralogical composition confirm the variable accuracy of sampling and the differentiation of petrophysical features of not only the deposit, but even a short interval in individual well sections [82]. The short distances between the wells and a small sampling depth interval preclude sedimentological analysis. The dominant mineral is dolomite. In the case of SEM determinations enabling "spatial" sampling, the dolomite contents obtained were clearly lower than those obtained by the XRD method. In the XRD method, the study concerns "flat sample", the visualization only dolomite (or another minerals) and porosity. To acquire comparable results, the dolomite contents obtained in SEM were converted to the solid phase (without porosity).

The percentage of dolomite varies from 79% (L1/1) to 95% (samples: 3, 4, 2, 1) (Tables 2 and 3). No relationship between depth and dolomite content was found. Gypsum and anhydrite are present in all samples. The content of these minerals also shows no correlation with increasing depth. The content of anhydrite in two samples (1; L1/1) was high and exceeded 15%. Plagioclase is present in all samples (several percent each, mostly albite), while samples L2/1 and L2/3 contain traces of quartz (at the detection limit). Traces of putative fluorite are found in sample L1/1.

4.2. Permeability Coefficient

The permeability study of the Main Dolomite using the mercury porosimeter indicates variable values. The mean permeability value is 35.27 mD, with a variation range from 0.9 to 135.6 mD. The samples come from a depth interval of 3283.80 to 3369.5 m. Samples 1 and 2 represent an interval between 3362 and 3370 m, where the permeability is generally low, with an average of 5.47 mD. Higher permeability values, up to 13.83 mD, are found in depth intervals of 3276.90–3277.00 and 3356.85–3361.30 m. The highest permeability value (k = 135.576 mD) was determined in a sample from a depth of 3357.32–3357.42 (Table 4). The variability in permeability values is also supported by the different porosities and mineralogical compositions. There is no change in permeability with depth, and there is no direct relationship between effective porosity and permeability (Figures 3 and 4).

Table 4. Permeability and porosity values of the Main Dolomite—Lubiatów deposit.

Sample No	Permeability Coefficient (mD)	Effective Porosity (%); Method—Porosimeter	Effective Porosity (%); Method—SEM	Depth (m)
L 2k/3	13.83	5.03		3356.85–3356.95
L 2k/5	135.58	21.14	18.66	3357.32–3357.42
L 2k/4	13.75	4.69	25.17	3361.20–3361.30
L 2k/2	7.40	12.58	15.16	3367.17–3367.27
L 2k/1	0.93	5.57		3369.50–3369.60
L 1/2	12.44		25.69	3273.35–3273.45
L 2/1	9.87		25.58	3274.32–3274.42
L 2/3	25.40		22.54	3275.85–3275.95
L 2/2	9.82		19.95	3276.90–3277.00
Average	25.45	9.80	23.00	Range 3273.35–3383.90
Max	135.58	4.69	15.16	
Min	7.40	21.14	31.21	

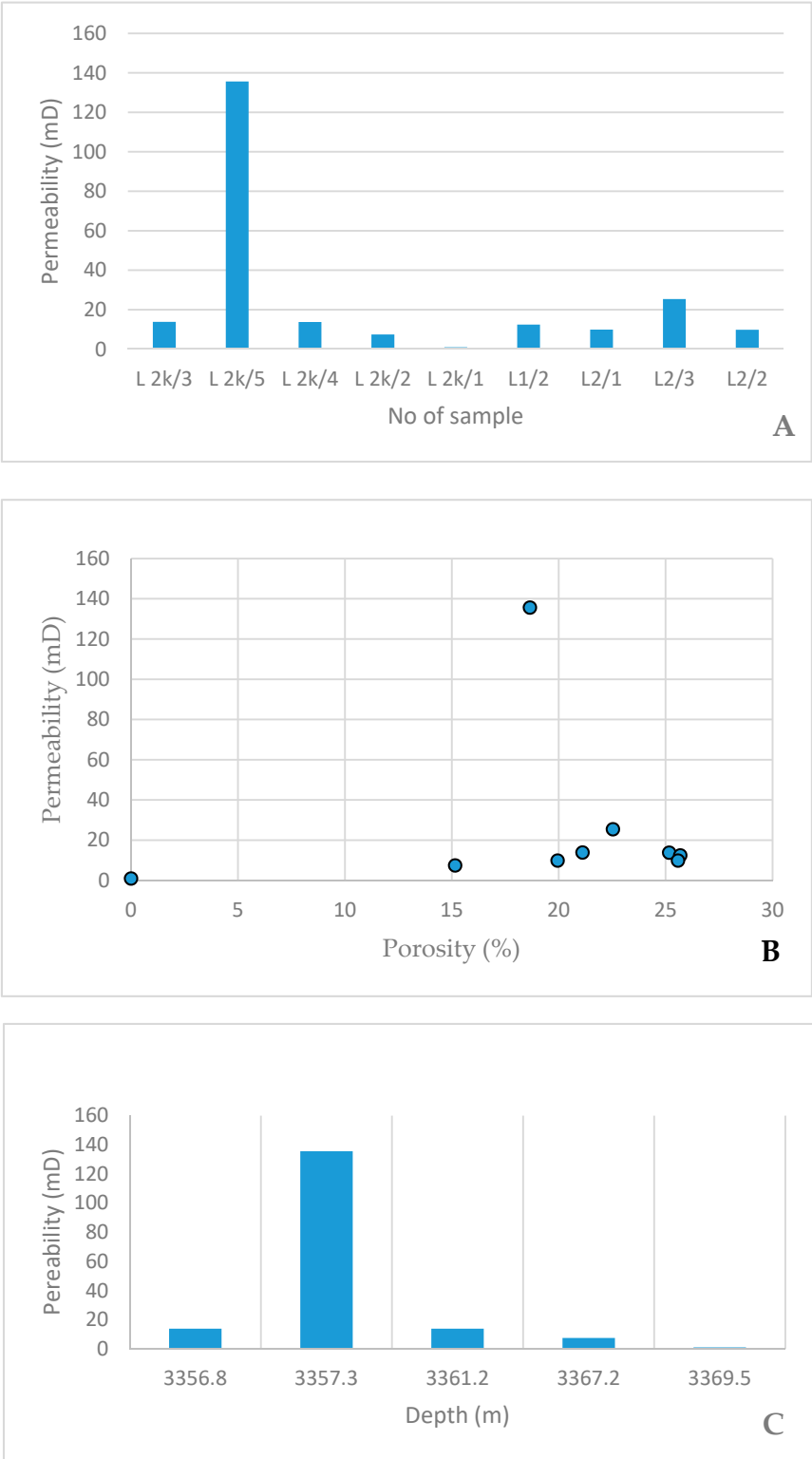

Figure 3. **A**—Value of permeability in all samples; **B**—permeability variation related to porosity; **C**—permeability variation to depth in L 2k.

5. Discussion

Porosity of the Main Dolomite of the Lubiatów deposit was investigated by the porosimetric method in the Oil and Gas Institute [25,83]. For the Well 1, Well 2 and Well 4 wells, the porosity was determined as the sum of effective porosity of the pore space and rock fracturing, ranging from

9.91% to 16.9%, respectively (Table 5). A major theme throughout the history of carbonate reservoir Ok research has been the effect of dolomitization on reservoir quality [11,84–87]. The results of research on dolomites from the Lubiatów deposit indicate no relationship between porosity and the identified lithofacies.

Table 5. Variability interval of porosity in the Main Dolomite subfacies in well sections [25,83].

Lithology	Effective Porosity (%)
Well 1	
Boundstones	0.29
Mudstones and wackestones	9.91
Packstones, grainstones, floatstones and rudstones	19.02
Well 2	
Mudstones and wackestones	3.88
Packstones, grainstones, floatstones and rudstones	19.50
Well 4	
Mudstones and wackestones	6.15
Packstones, grainstones, floatstones and rudstones	12.57

Studies of carbonate platforms in the Bahamas and Marion Plateau show evidence of major heterogeneity in porosity and permeability related of depositional texture and eogenetic diagenesis. Certainly, these factors are responsible for the wide heterogeneity [86].

Parameterization of porosity-dependent permeability has been the subject of many studies. There is a noticeable variation in the porosity of dolomites even within a single deposit or its part [8–10,88,89].

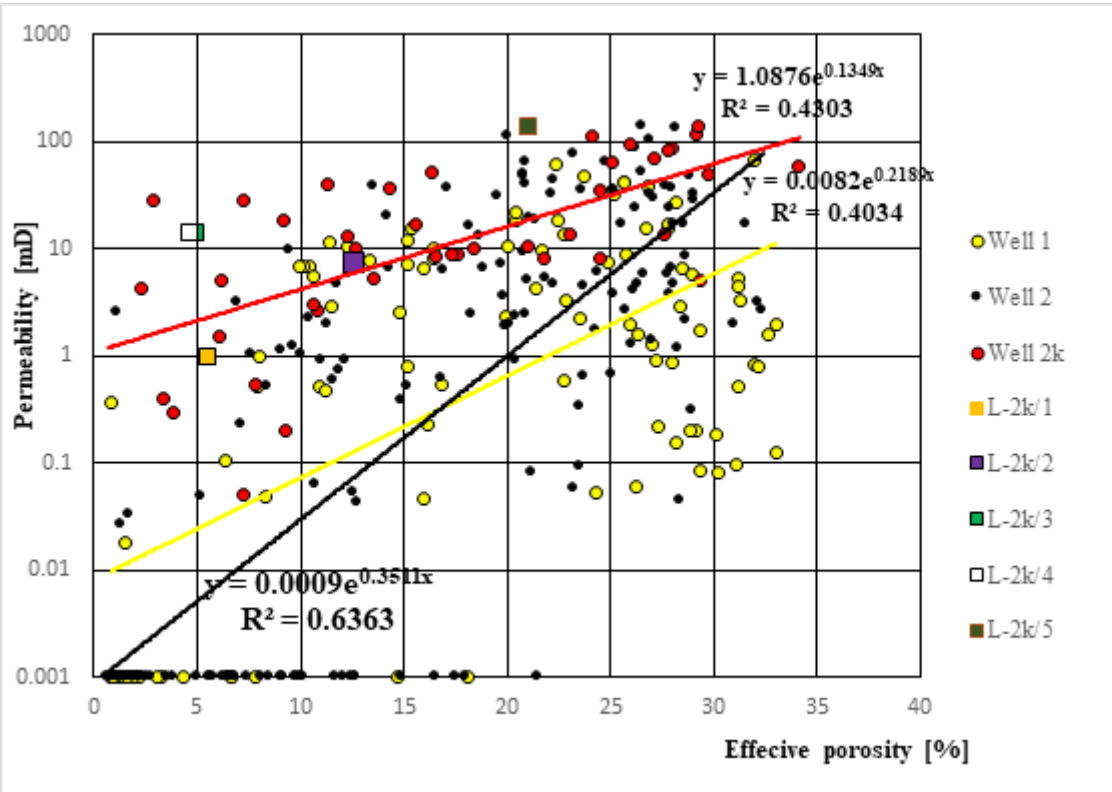

Figure 4. Relationship between effective porosity and permeability ([24,25,90] and this work L 2k).

Due to the complicated rock textures and overlapping alteration processes, including secondary crystallization or dissolution of minerals, the permeability of rocks in the Lubiatów deposit is variable. The research on the relationship between porosity and permeability was carried out for more than 2500 samples of the Main Dolomite from the Polish Lowlands. The value of the linear correlation coefficient was calculated to be R = 0.21 [25], confirming the diversity of the deposit and the lack of relationship between porosity and permeability.

The permeability in the Well 1 and 2, determined in this work, is 7.48 and 12.79 mD, respectively (Tables 4 and 5), while the permeability determined on the basis of flow tests (based on formation pressure build-up) was 13.94 and 71 mD, respectively, at a test range covering up to 125 m of the well section [24,25,90]. The differences are due to many reasons i.e., micro fractures, the differentiation of the mineralogical composition, sedimentological processes, the location of the well and account for horizontal and vertical permeability. The differentiation confirms the need for direct research and recommends great caution when accepting data from other wells in interpretations. The permeability determined by the laboratory method in individual wells is lower than the permeability determined as a result of flow tests. This results from the presence of the so-called fracture permeability in the rock mass, ignored in laboratory tests that, however, determine petrophysical features precisely at a specific depth. The problem of the differentiation of conductivity results determined in laboratory tests and in-situ conditions and the possibility of comparing the results has been the subject of many publications (among others [91]).

The Pekisko Formation in the Bigoray field in central Alberta is an oil-bearing dual permeability/porosity dolomite, a part of the reservoir has permeabilities in the range of 1–2 Darcy and porosities approaching 25–30%, while the rest of the reservoir features 10–30 millidarcy average permeabilities, 8–12% porosities, and low initial water saturation [92]. Permeability in the range of 1–2 Darcy accompanied by high porosity can be considered as fracture permeability.

The varying permeability in the well (Figures 4 and 5) confirms the depth-related variability in petrophysical features of the deposit, without a definite trend.

In geological modelling studies of the Ca2 deposit (about 300 km^2), the fracture and intergranular porosity distribution was determined on the basis of porosity measurements in laboratory tests. Modelling studies that are based on data from the distribution of discrete values in 978,950 cells of the model yielded the porosity distribution from 0% to 32%, with an average value of 8% [23]. The permeability model was developed in the same way as the porosity model. Data from 1208 laboratory determinations performed on 13 wells for four facies were used. The fracture permeability model was developed on the basis of 282 laboratory measurements. The mean values resulting from the modelling process indicate permeability values ranging from 0 to 192 mD, with an average value of 7 mD [30]. The greatest fracture permeability is found in the middle of the sections, in the zones of rapid change of the gradient of the top of the Main Dolomite, and at the barrier/platform slope boundary. This work does not confirm the results averaged from the geological model. The model is a result of many elements, of the applied schematization, and the calculation algorithm used; it is a schematic diagram of geological conditions, enabling spatial, regional characterization of the deposit. The data from the model characterize the spatial, regional variability of parameters.

The permeability values obtained in laboratory tests (mercury porosimeter) were compared with the results of other studies of dolomites in other deposits, including the North Field, USA [93–95], Jiannan area, Eastern Sichuan Basin, China [66], Pre-Caspian Basin [4], West Texas Dolomite [94] and Upper Jurassic carbonate rock of the Malm reservoir in the South German Molasse Basin [96]. It is practically unnecessary to directly compare the results of permeability different rocks from different depth, lithology or measurements methodology. The permeability value is varied, which confirms the effect of many factors on the permeability. Dolomite is a rock of low permeability that varies between individual deposits and between different parts of the same deposit. This supports the need for direct research and limits the use of correlation relationships with other parameters.

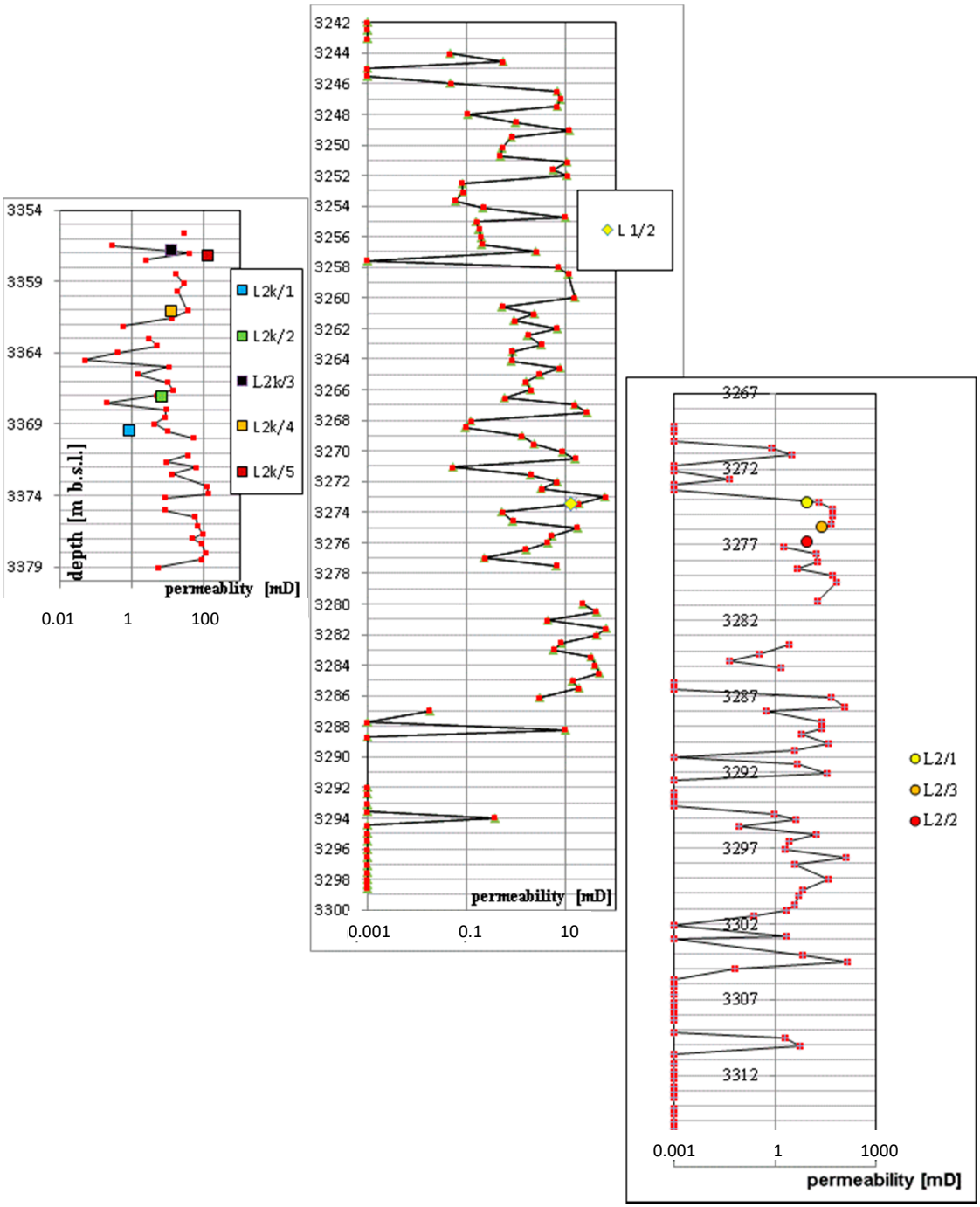

Figure 5. Permeability of dolomites from the Well 2k (L2k), Well 1 (L1) and Well 2 (L2) wells ([24,25,90] and this work).

6. Conclusions

The permeability of dolomites depends largely on facies variability, mineralogical composition, pore-space features (including predominantly the size and geometry of pores), fracture opening, and pore specific surface area. There is no correlation between permeability and petrophysical and geological features that have an integrated and cumulative effect on the magnitude of permeability. Both this work and those based on historical data show no relationships between the porosity and permeability, depth and mineral composition of dolomites.

Dolomite, which is a reservoir rock for hydrocarbons in the Polish Lowlands, is characterized by a varied mineralogical composition and variable permeability and porosity values. The studies of dolomites from a depth of 3242–3380 m show a considerable variability in mineralogical composition. The content of dolomite ranges from 76% to 97%, the content of anhydrite varies from 0.67% to 19.43%, the amounts of gypsum and quartz are from traces to 19.43%, and there is also quartz (at the detection limit) to over 5% and traces of fluorite, plagioclases and clay minerals. The porosity ranged from 4.69% to 31.21%, depending on the measurement method used. The average permeability value is 35.27 mD, with a variation range from 0.9 to 135.6 mD within the entire drilling interval.

The various methods of studying permeability of the Lubiatów hydrocarbon deposit yielded different results. They confirm heterogeneity of the deposit in terms of permeability and the need to select the research methodology depending on the study purpose of the analysis. Regional studies present a permeability model, while detailed laboratory tests enable measuring permeability at a specific drilling depth, which allows, among other things, forecasting the inflow of hydrocarbons to the wellbore, selecting the method of wellbore treatment, and planning drilling techniques. In practice, the use of databases of petrophysical properties of dolomite from other deposits is risky in forecasting permeability values, which results from the influence of many factors and their characteristics on the permeability of dolomites. We join the call, initiated by Ehrenberg and Nadeau [45], to present data with a broad methodological description and information on depth and characteristics of reservoir rocks to create a research database for application purposes in the oil industry.

Author Contributions: Conceptualization, E.K.; Methodology, E.K., K.S., S.Z., E.F.; Formal Analysis, E.K., K.S., S.Z., E.F.; Investigation, K.S., S.Z., E.F.; Resources, E.K., K.S., S.Z., E.F.; Writing E.K., S.Z. Original Draft Preparation, E.K.; Writing—Review and Editing, E.K., K.S., S.Z., E.F.; Visualization, E.K., K.S., S.Z.; Project Administration, E.K. All authors have read and agreed to the published version of the manuscript.

Funding: This research received no external funding.

Conflicts of Interest: The authors declare no conflict of interest.

References

1. Jarzyna, J.; Ujma, P. Wyznaczanie przepuszczalności skał klastycznych czerwonego spągowca z wykorzystaniem sztucznych sieci neuronowych. *Naft. Gaz* **2012**, *2*, 85–96. (In Polish)
2. Tucker, M.E. *Sedimentary Rocks in the Field*; John Wiley & Sons: Chichester, UK, 2003; p. 234.
3. Zitong, Q. *Carbonate Reservoir Geology*; China University of Petroleum Press: Dongying, China, 2007; pp. 32–78.
4. He, L.; Zhao, L.; Li, J.; Ma, J.; Lui, R.; Wang, S.; Zhao, W.-Q. Complex relationship between porosity and permeability of carbonate reservoirs and its controlling factors: A case study of platform facies in Pre-Caspian Basin. *Pet. Explor. Dev.* **2014**, *41*, 225–234. [CrossRef]
5. Zhao, W.; Shen, A.; Zhou, J.; Wang, X.; Lu, J. Types, characteristics, origin and exploration significance of reef-shoal reservoirs: A case study of Tarim Basin, NW China and Sichuan Basin, SW China. *Pet. Explor. Dev.* **2014**, *41*, 283–293. [CrossRef]
6. Ruzyla, K.; Friedman, G.M. Geological Heterogeneities Important to Future Enhanced Recovery in Carbonate Reservoirs of Upper Ordovician Red River Formation at Cabin Creek Field, Montana. *Soc. Pet. Eng. J.* **1982**, *22*, 429–444. [CrossRef]
7. Ruzyla, K.; Friedman, G.M. Factors controlling porosity in dolomite reservoirs of the Ordovician Red River Formation, Cabin Creek Field Montana. In *Carbonate Petroleum Reservoirs*; Roehl, P.O., Choquette, P.W., Eds.; Springer: New York, NY, USA, 1985; pp. 39–58. ISBN 978-1-4612-9536-5.
8. Bebout, D.; Lucia, G.; Hocott, C.R.; Fogg, G.E.; Van der Stoep, G.W. Characterization of the Grayburg reservoir, University Lands Dune field, Crane County, Texas. In *Report of Investigations*; University of Texas, Bureau of Economic Geology: Austin, TX, USA, 1987; Volume 168, p. 104.
9. Major, R.P.; Holtz, M.H. Predicting reservoir quality at the development scale: Methods for quantifying remaining hydrocarbon resource in diagenetically complex carbonate reservoirs. In *Reservoir Quality Prediction in Sandstones and Carbonates*, 1st ed.; Kupecz, J.A., Bloch, S., Gluyas, J., Eds.; AAPG Memoir: Tulsa, OK, USA, 1997; Volume 69, pp. 231–248. ISBN 9781629810799.

10. Kerans, F.J.L.C. Integrated Characterization of Carbonate Ramp Reservoirs Using Permian San Andres Formation Outcrop Analogs. *Aapg Bull.* **1994**, *78*, 181–216. [CrossRef]
11. Sun, D.; Liu, D.; Chen, M.; An, Z.; John, S. Magnetostratigraphy and palaeoclimate of Red Clay sequences from Chinese Loess Plateau. *Sci. China Ser. D Earth Sci.* **1997**, *40*, 337–343. [CrossRef]
12. Semyrka, R. Uwarunkowania roponośności dolomitu głównego na obszarze Pomorza Zachodniego. *Pr. Geol. Pan* **1995**, *129*, 5–113. (In Polish)
13. Scheirer, A.H. *Petroleum Systems and Geologic Assessment of Oil and Gas in the San Joaquin Basin Province, California*; U.S. Geological Survey Professional Paper; U.S. Geological Survey: Reston, VA, USA, 2007; p. 1713. Available online: http://pubs.usgs.gov/pp/pp1713/ (accessed on 20 October 2020).
14. Pikulski, L. Analiza paleogeograficzna utworów dolomitu głównego (Ca2) w rejonie Lubiatów—Międzychód—Grotów w aspekcie poszukiwania złóż. *Naft. Gaz* **2004**, *9*, 397–405. (In Polish)
15. Forsal.pl. Available online: https://forsal.pl/artykuly/692558,pgnig-kopalnia-lubiatow-miedzychod-grotow-rozpoczyna-wydobycie.html (accessed on 20 October 2020).
16. Gautier, D.L. Carboniferous-Rotliegend total petroleum system description and assessment results summary. *U.S. Geol. Surv. Bull.* **2003**, *2211*, 24.
17. Karnkowski, P.H. Petroleum Provinces in Poland. *Przegląd Geol.* **2007**, *55*, 1061–1067. (In Polish)
18. Polish Geological Institute—National Research Institute. Bilans Zasobów Złóż Kopalin w Polsce według stanu na 31 XII 2018 r. Available online: http://geoportal.pgi.gov.pl/css/surowce/images/2018/pdf/bilans_2018.pdf (accessed on 20 October 2020). (In Polish)
19. Sokołowski, J.; Tomaszewski, A. *Atlas Geosynoptyki Naftowej Polski 1: 2,500,000, 1: 1,000,000, 1:500,000*; Wydawnictwo Geologiczne: Warsaw, Poland, 1988. (In Polish)
20. Wagner, R. Stratygrafia osadów i rozwój basenu cechsztyńskiego na Niżu Polskim. *Pr. Pa%C584stwowego Inst. Geol.* **1994**, *146*, 1–71, (In Polish with English Summary and Figure Captions).
21. Wagner, R.; Kotarba, M. Generation potential of the Zechstein Main Dolomite (Ca2) carbonates in the Gorzów Wielkopolski-Miedzychód-Lubiatów area: Geological and geochemical approach to microbial-algal source rock. *Przegląd Geol.* **2007**, *55*, 1025–1036.
22. Jaworowski, K.; Mikołajewski, Z. Oil- and gas-bearing sediments of the Main Dolomite (Ca2) in the Międzychód region: A depositional model and the problem of the boundary between the second and third depositional sequences in the Polish Zechstein Basin. *Przegląd Geol.* **2007**, *55*, 1017–1024.
23. Papiernik, B.; Machowski, G.; Słupczyński, K.; Semyrka, R. Geologiczny model rejonu akumulacji ropno-gazowej Lubiatów-Międzychód-Grotów (LMG). *Geologia* **2009**, *35*, 175–182. (In Polish)
24. Semyrka, R. *Facjalno-strukturalne uwarunkowania akumulacji węglowodorów dolomitu głównego (Ca2) w granicznej strefie platformy węglanowej w obszarze Gorzów-Pniewy*; A research grant; NCN Kraków: Cracow, Poland, 2012. (In Polish)
25. Semyrka, R.; Jarzyna, J.A.; Krakowska, P.I.; Semyrka, G. Analiza statystyczna parametrów mikrofacji dolomitu głównego w granicznej strefie platformy węglanowej. *Miner. Resour. Manag.* **2015**, *31*, 123–140. [CrossRef]
26. Peryt, T. Sedimentology and paleoecology of the Zechstein limestone (upper Permian) in the fore-sudetic area (Western Poland). *Sediment. Geol.* **1978**, *20*, 217–243. [CrossRef]
27. Antonowicz, L.; Knieszner, L. Zechstein reefs of the Main Dolomite in Poland and their seismic recognition. *Acta Geol. Pol.* **1984**, *34*, 81–94.
28. Głowacki, E. Uwagi dotyczące rozwoju dolomitu głównego i jego znaczenie dla poszukiwań naftowych w rejonie Poznania. *Nafta* **1986**, *42*, 304–309. (In Polish)
29. Knieszner, L.; Protas, A. Próba określenia zasięgów litofacjalnych dolomitu głównego w rejonie Rymań-Piaski-Ciechnowo-Świdwin-Rosnowo. In Proceedings of the Science and Technology Conference "Rozwój poszukiwań węglowodorów w północno-zachodniej Polsce w okresie 40-lecia działalności Zakładu Poszukiwania Nafty i Gazu w Pile (1956–1996) oraz perspektywy dalszych odkryć", Piła, Poland, 17–18 April 1996; Arch. Geonafta: Warsaw, Poland, 1996. (In Polish)
30. Jarzyna, J.; Puskarczyk, E.; Bała, M.; Papiernik, B. Variability of the Rotliegend sandstones in the Polish part of the Southern Permian Basin–permeability and porosity relationships. *Ann. Soc. Geol. Pol.* **2009**, *79*, 13–26.
31. Pikulski, L. Sedymentacja oraz rozwój litofacjalny utworów dolomitu głównego w rejonie złoża BMB, zachodnia Polska. *Przegląd Geol.* **1998**, *46*, 426–435. (In Polish)

32. Szczawińska, I. *Dodatek nr 1 do Dokumentacji geologicznej złoża ropy naftowej "Lubiatów"*; PGNiG S.A. Ośr; Północ: Piła, Poland, 2004. (In Polish)
33. Polish Oil and Gas Company S.A. Available online: http://pgnig.pl (accessed on 20 October 2020).
34. Kwolek, K.; Mikołajewski, Z. Kryteria identyfikacji obiektów litofacjalnych jako potencjalnych pułapek złożowych w utworach dolomitu głównego (Ca2) u podnóża platform i mikroplatform węglanowych w środkowo-zachodniej Polsce. *Przegląd Geol.* **2010**, *58*, 426–435. (In Polish)
35. Journal of Laws. 2020. Available online: https://isap.sejm.gov.pl/isap.nsf/download.xsp/WDU20111630981/U/D20110981Lj.pdf (accessed on 20 October 2020).
36. Archie, G.E. The Electrical Resistivity Log as an Aid in Determining Some Reservoir Characteristics. *Trans. Aime* **1942**, *146*, 54–62. [CrossRef]
37. Wharton, R.P.; Hazen, G.A.; Rau, R.N.; Best, D.L. Electromagnetic propagation logging: Advances in technique and interpretation. In Proceedings of the SPE Annual Technical Conference and Exhibition, Dallas, TX, USA, 21–24 September 1980; Society of Petroleum Engineers: Dallas, TX, USA, 1980; p. 9267.
38. Borai, A. A New Correlation for the Cementation Factor in Low-Porosity Carbonates. *Soc. Pet. Eng.* **1987**, *2*, 495–499. [CrossRef]
39. Lines, L.R.; Schultz, A.K.; Treitel, S. Cooperative inversion of geophysical data. *Geophysics* **1988**, *53*, 8–20. [CrossRef]
40. Schön, J.H. Physical properties of rocks—Fundamental and principles of petrophysics. In *Handbook of Geophysical Exploration, Seismic Exploration*; Helbig, K., Treitel, S., Eds.; Pergamon Press: London, UK, 1996; Volume 18, p. 583.
41. Pride, S.R. Relationships between seismic and hydrological properties. In *Hydrogeophysics*; Rubin, Y., Hubbard, S.S., Eds.; Springer: Dordrecht, The Netherlands, 2005; pp. 87–128.
42. Herzig, J.; Szczepańska, J. Zastosowanie metody flow-pump do badań współczynnika filtracji w gruntach słabo przepuszczalnych. In *Współczesne Problemy Hydrogeologii VII, Kraków-Krynica, Poland*; AGH: Cracow, Poland, 1995. (In Polish)
43. Bukowski, P.; Niedbalska, K.; Augustyniak, A.; Haładus, A.; Kura, K.; Małaszuk, T. Zastosowanie wybranych metod badań masywów skalnych do oceny warunków hydrogeologicznych kopalń węgla kamiennego GZW. *Przegląd Geol.* **2017**, *65*, 933–937. (In Polish)
44. Zawisza, L. Simplified method of absolute permeability estimation of porous beds. *Arch. Min. Sci.* **1993**, *38*, 343–352.
45. Ehrenberg, S.N.; Nadeau, P.H. Sandstone vs. carbonate petroleum reservoirs: A global perspective on porosity-depth and porosity-permeability relationships. *AAPG Bull.* **2005**, *89*, 435–445. [CrossRef]
46. Aguilera, R. Sandstone vs. carbonate petroleum reservoirs: A global perspective on porosity-depth and porosity-permeability relationships: Discussion. *AAPG Bull.* **2006**, *90*, 807–810. [CrossRef]
47. Xiao, Z.X.; Xiao, L. Method to calculate reservoir permeability using nuclear magnetic resonance logging and capillary pressure data. *Atom. Energy Sci. Technol.* **2008**, *42*, 868–971. (In Chinese)
48. Xiao, L.; Liu, X.P.; Zou, C.C.; Hu, X.X.; Mao, Z.Q.; Shi, Y.J.; Guo, H.P.; Li, G.R. Comparative study of models for predicting permeability from nu-clear magnetic resonance (NMR) logs in two Chinese tight sandstone reservoirs. *Acta Geophys.* **2014**, *62*, 116–141. [CrossRef]
49. Jiang, G.; Ni, X.; Yang, L.; Li, W.; Li, Y.; Deng, Z. Synthesis of superamphiphobic nanofluid as a multi-functional additive in oil-based drilling fluid, especially the stabilization performance on the water/oil interface. *Colloids Surf. A Phys. Eng. Asp.* **2020**, *588*, 124385. [CrossRef]
50. Hsieh, P.A.; Tracy, J.V.; Neuzil, C.E.; Bredehoeft, J.D.; Silliman, S.E. A transient laboratory method for determining the hydraulic properties of 'tight' rocks: I. Theory. *Int. J. Rock Mech. Min. Sci.* **1981**, *18*, 245–252. [CrossRef]
51. Bliefnick, J.G.K.D.M. Pore Geometry: Control on Reservoir Properties, Walker Creek Field, Columbia and Lafayette Counties, Arkansas. *AAPG Bull.* **1996**, *80*, 1027–1044. [CrossRef]
52. Melas, F.F.; Friedman, G.M. Petrophysical Characteristics of the Jurassic Smackover Formation, Jay Field, Conecuh Embayment, Alabama and Florida (1). *AAPG Bull.* **1992**, *76*, 81–100. [CrossRef]
53. Cui, X.; Bustin, R.; Dipple, G.M. Selective transport of CO2, CH4, and N2 in coals: Insights from modeling of experimental gas adsorption data. *Fuel* **2004**, *83*, 293–303. [CrossRef]

54. Timur, A. Nuclear magnetic resonance study of carbonate rocks. In Proceedings of the SPWLA 13th Annual Logging Symposium, Tulsa, OK, USA, 7–10 May 1972; Society of Petrophysicists and Well-Log Analysts: Tulsa, OK, USA, 1972.
55. Chang, M.-H.; Chen, F.; Straughan, B. Instability of Poiseuille flow in a fluid overlying a porous layer. *J. Fluid Mech.* **2006**, *564*, 287–303. [CrossRef]
56. Wells, J.D.; Amaefule, J.O. Capillary Pressure and Permability Relationships in Tight Gas Sands. In Proceedings of the SPE DOE Low Permeability Gas Reservoirs Symposioum, Denver, CO, USA, 19–22 March 1985; Society of Petroleum Engineers: Fort Worth, TX, USA.
57. Comisky, J.T.; Santiago, M.; McCollom, B.; Buddhala, A.; Newsham, K.E. Sample Size Effects on the Application of Mercury Injection Capillary Pressure for Determining the Storage Capacity of Tight Gas and Oil Shales. In Proceedings of the Canadian Unconventional Resources Conference, Calgary, AB, Canada, 15–17 November 2011; Society of Petroleum Engineers: Calgary, AB, Canada, 2011.
58. Zhang, Z.; Shi, Y.; Li, H.; Jin, W. Experimental study on the pore structure characteristics of tight sandstone reservoirs in Upper Triassic Ordos Basin China. *Energy Explor. Exploit.* **2016**, *34*, 418–439. [CrossRef]
59. Weyl, P.K. Porosity Through Dolomitization: Conservation-Of-Mass Requirements. *J. Sediment. Res.* **1960**, *30*, 85–90. [CrossRef]
60. Schmoker, R.B.H.J.W. Carbonate Porosity Versus Depth: A Predictable Relation for South Florida. *AAPG Bull.* **1982**, *66*, 2561–2570. [CrossRef]
61. Lucia, F.J.; Major, R.P. Porosity evolution through hypersaline reflux dolomitization. In *Dolomites: A Volume in Honour of Dolomieu, Proceedings of the Dolomieu Conference on Carbonate Platforms and Dolomitization, Ortisei, Italy, September 1991*; Purser, B., Tucker, M., Zenger, D., Eds.; Blackwell Scientific Publications: Boston, MA, USA, 1994.
62. Chatzis, I.; Dullien, F.A.L. The modeling of mercury porosimetry and the relative permeability of mercury in sandstones using percolation theory. *Int. Chem. Eng.* **1985**, *25*, 21.
63. Ioannidis, M.A.; Chatzis, I. A Mixed-Percolation Model of Capillary Hysteresis and Entrapment in Mercury Porosimetry. *J. Colloid Interface Sci.* **1993**, *161*, 278–291. [CrossRef]
64. Fang, X.; Cai, Y.; Liu, D.; Zhou, Y. A Mercury Intrusion Porosimetry Method for Methane Diffusivity and Permeability Evaluation in Coals: A Comparative Analysis. *Appl. Sci.* **2018**, *8*, 860. [CrossRef]
65. Washburn, E.W. The Dynamics of Capillary Flow. *Phys. Rev.* **1921**, *17*, 273–283. [CrossRef]
66. Wang, Q.; Li, W.; Zhang, D.; Wang, H.; Jiang, W.; Zhu, L.; Tao, J.; Huo, P.; Zhang, J. Influence of high-pressure CO_2 exposure on adsorption kinetics of methane and CO_2 on coals. *J. Nat. Gas Sci. Eng.* **2016**, *34*, 811–822. [CrossRef]
67. Cai, Y.; Liu, D.; Pan, Z.; Che, Y.; Liu, Z. Investigating the Effects of Seepage-Pores and Fractures on Coal Permeability by Fractal Analysis. *Transp. Porous Media* **2015**, *111*, 479–497. [CrossRef]
68. Micromeritics' AutoPore IV 9500 Series. Available online: https://www.micromeritics.com/product-showcase/autopore-iv.aspx?no_redirect=true (accessed on 20 October 2020).
69. Thomeer, J. Air Permeability as a Function of Three Pore-Network Parameters. *J. Pet. Technol.* **1983**, *35*, 809–814. [CrossRef]
70. Swanson, B.F. Properties of porous media affecting fluid flow. *J. Irrig. Drain. Eng.* **1966**, *92*, 61–88.
71. Jones, F.O.; Owens, W.W. A Laboratory Study of Low-Permeability Gas Sands. *J. Pet. Technol.* **1980**, *32*, 1631–1640. [CrossRef]
72. Carles, P.; Egermann, P.; Lenormand, R.; Lombard, J.M. Low Permeability Measurements Using Steady-State and Transient Methods. In Proceedings of the International Symposium of the Society of Core Analysts, Calgary, AB, Canada, 10–12 September 2007.
73. Bustin, R.M. Petroleum source rocks, organic maturation and thermal history of the Queen Charlotte Basin, British Columbia. *Bull. Can. Pet. Geol.* **1997**, *45*, 255–278.
74. Bustin, R.M.; Bustin, A.M.; Cui, A.; Ross, D.; Pathi, V.M. Impact of Shale Properties on Pore Structure and Storage Characteristics. In Proceedings of the SPE Shale Gas Production Conference, Fort Worth, TX, USA, 16–18 November 2008; Society of Petroleum Engineers (SPE): Fort Worth, TX, USA, 2008.
75. Katz, A.J.; Thompson, A.H. Quantitative prediction of permeability in porous rock. *Phys. Rev. B* **1986**, *34*, 8179–8181. [CrossRef]
76. Katz, A.J.; Thompson, A.H. Prediction of rock electrical conductivity from mercury injection measurements. *J. Geophys. Res. Space Phys.* **1987**, *92*, 599–607. [CrossRef]

77. Pittman, E.D. Porosity and Permeability Changes During Diagenesis of Pleistocene Corals, Barbados, West Indies. *Geol. Soc. Am. Bull.* **1974**, *85*, 1811. [CrossRef]
78. Such, P. An Application of Fractal Analysis in Investigations of Reservoir Rocks. In Proceedings of the Conference and Exhibition: Modern Exploration and Improved Oil and Gas Recovery Methods, Cracow, Poland, 1–4 April 1998.
79. Such, P. Wykorzystanie porometrii rtęciowej w analizie przestrzeni porowej skał zbiornikowych. *Pr. Ignig* **2002**, *113*, 86. (In Polish)
80. Webb, P.A. *An Introduction to the Physical Characterization of Materials by Mercury Intrusion Porosimetry with Emphasis on Reduction and Presentation of Experimental Data*; Micromeritics Instrument Corporation: Norcross, GA, USA, 2001.
81. Gao, Z.; Hu, Q. Estimating permeability using median pore-throat radius obtained from mercury intrusion porosimetry. *J. Geophys. Eng.* **2013**, *10*, 025014. [CrossRef]
82. Krogulec, E.; Sawicka, K.; Zabłocki, S. Hydrogeochemical modelling of water injection into an oil and gas well under high-pressure high-temperature (HPHT) conditions. *Acta Geol. Pol.* **2020**, *70*, 419–433.
83. Semyrka, R.; Semyrka, G.; Zych, I. Zmienność parametrów petrofizycznych subfacji dolomitu głównego zachodniej strefy półwyspu Grotowa w świetle badań porozymetrycznych. *Geologia* **2008**, *34*, 445–468. (In Polish)
84. Moore, C.H. *Carbonate Reservoirs Porosity Evolution and Diagenesis in a Sequence Stratigraphic Framework*, 1st ed.; Elsevier: Amsterdam, The Netherlands, 2001; p. 444.
85. Braithwaite, C.J.; Rizzi, G.; Darke, G. The geometry and petrogenesis of dolomite hydrocarbon reservoirs: Introduction. *Geol. Soc.* **2004**, *235*, 1–6. [CrossRef]
86. Ehrenberg, S.N.; Eberli, G.P.; Keramati, M.; Moallemi, A. Permeability-porosity relationships in interbedded limestone-dolostone reservoirs. *AAPG Bull.* **2006**, *90*, 91–114. [CrossRef]
87. Ehrenberg, S.N.; Walderhaug, O.; Bjørlykke, K. Carbonate porosity creation by mesogenetic dissolution: Reality or illusion? *AAPG Bull.* **2012**, *96*, 217–233. [CrossRef]
88. Borer, J.M.; Harris, P.M. Lithofacies and Cyclicity of the Yates Formation, Permian Basin: Implications for Reservoir Heterogeneity (1). *AAPG Bull.* **1991**, *75*, 726–779. [CrossRef]
89. Cowan, P.M.H.P.E. Porosity Distribution in San Andres Formation (Permian), Cochran and Hockley Counties, Texas. *AAPG Bull.* **1986**, *70*, 888–897. [CrossRef]
90. Kaźmierczuk, M.; Jarzyna, J.; Semyrka, R. Wykorzystanie analizy składowych głównych do opracowania parametrów zbiornikowych w rejonie złóż Międzychód, Sieraków, Sowia Góra, Grotów i Lubiatów. *Tech. Poszuk. Geol.* **2006**, *2*, 57–63. (In Polish)
91. Erkan, K. *A Comparative Overview of Geophysical Methods*; Raport No. 488; The Ohio State University: Columbus, OH, USA, 2008; p. 66. Available online: https://core.ac.uk/download/pdf/159585702.pdf (accessed on 20 October 2020).
92. Warren, J. Dolomite: Occurrence, evolution and economically important associations. *Earth-Sci. Rev.* **2000**, *52*, 1–81. [CrossRef]
93. Allan, J.R.; Wiggins, W.D. *Dolomite Reservoirs. Geochemical Techniques for Evaluating Origin and Distribution*; American Association of Petroleum Geologists: Tulsa, OK, USA, 1993; Volume 36, p. 129.
94. Henderson, N.; Saller, A.H. Distribution of Porosity and Permeability in Platform Dolomites: Insight from the Permian of West Texas. *AAPG Bull.* **1998**, *82*, 1528–1550. [CrossRef]
95. Repl, D.D.W.M. Distribution of porosity and permeability in platform dolomites: Insight from the Permian of west Texas (Discussion & Reply). *AAPG Bull.* **2001**, *85*, 525–532. [CrossRef]
96. Bohnsack, D.; Potten, M.; Pfrang, D.; Wolpert, P.; Zosseder, K. Porosity–permeability relationship derived from Upper Jurassic carbonate rock cores to assess the regional hydraulic matrix properties of the Malm reservoir in the South German Molasse Basin. *Geotherm. Energy* **2020**, *8*, 1–47. [CrossRef]

Publisher's Note: MDPI stays neutral with regard to jurisdictional claims in published maps and institutional affiliations.

© 2020 by the authors. Licensee MDPI, Basel, Switzerland. This article is an open access article distributed under the terms and conditions of the Creative Commons Attribution (CC BY) license (http://creativecommons.org/licenses/by/4.0/).